HHS Public Access

Author manuscript

Neurobiol Dis. Author manuscript; available in PMC 2021 June 01.

Published in final edited form as:

Neurobiol Dis. 2020 June ; 139: 104819. doi:10.1016/j.nbd.2020.104819.

Directional deep brain stimulation leads reveal spatially distinct oscillatory activity in the globus pallidus internus of Parkinson's disease patients

Joshua E. Aman, PhD[a,*], **Luke A. Johnson, PhD**[a,*], **David Escobar Sanabria, PhD**[a], **Jing Wang, PhD**[a], **Remi Patriat, PhD**[b], **Meghan Hill**[a], **Ethan Marshall**[a], **Colum D. MacKinnon, PhD**[a], **Scott E. Cooper, MD, PhD**[a], **Lauren E. Schrock, MD**[a], **Michael C. Park, MD PhD**[c], **Noam Harel, PhD**[b,c], **Jerrold L. Vitek, MD PhD**[+,a]

[a]Department of Neurology, University of Minnesota, 516 Delaware Street SE, 12-100 Phillips Wangensteen Building, Minneapolis, Minnesota, USA

[b]Center for Magnetic Resonance Research, Department of Radiology, University of Minnesota, 20216th Street SE, Minneapolis, Minnesota, USA

[c]Department of Neurosurgery, University of Minnesota, 420 Delaware Street SE, Minneapolis, Minnesota, USA

Abstract

The goal of this study was to characterize the spectral characteristics and spatial topography of local field potential (LFP) activity in the internal segment of the globus pallidus (GPi) in patients with Parkinson's disease utilizing directional (segmented) deep brain stimulation (dDBS) leads. Data were collected from externalized dDBS leads of three patients with idiopathic Parkinson's disease after overnight withdrawal of parkinsonian medication at rest and during a cued reach-to-

[+]Corresponding Author: Jerrold L. Vitek, vitek004@umn.edu, Neurology Department, 12-100 PWB, 516 Delaware St SE, Minneapolis, MN 55455, +1 612-624-1903.

[*]authors contributed equally to this work

CRediT author statement

1. Conceptualization
2. Methodology
3. Software
4. Validation
5. Formal Analysis
6. Investigation
7. Resources
8. Data Curation
9. Writing – Original Draft
10. Writing – Review & Editing
11. Visualization
12. Supervision
13. Project administration
14. Funding acquisition

Joshua E. Aman: 2,3,4,6,7,8,9,10,11,12,13; **Luke A. Johnson:** 2,3,4,5,6,7,8,9,10,11,12,13; **David Escobar Sanabria:** 2,3,4,6,7,8,9,10,11,12,13; **Jing Wang:** 2,3,4,6,7,8,9,10,11,12,13; **Remi Patriat:** 2,3,4,5,6,7,8,10,11; **Meghan Hill:** 6,7,8,11; **Ethan Marshall:** 6,7,8; **Colum D. MacKinnon:** 1,2,7,10,12; **Scott E. Cooper:** 2,6,7,10,12; **Lauren E. Schrock:** 2,6,7,10,12; **Michael C. Park:** 1,2,6,7,10,12,13; **Noam Harel:** 1,2,3,4,5,6,7,8,10,11,12,13,14; **Jerrold L. Vitek:** 1,2,6,7,8,9,10,11,12,13,14

target task. Oscillatory activity across lead contacts/segments was examined in the context of lead locations and contact orientations determined using co-registered preoperative 7 Tesla (T) MRI and postoperative CT scans. Each of the three patients displayed a unique frequency spectrum of oscillatory activity in the pallidum, with prominent peaks ranging from 5 to 35Hz, that modulated variably across subjects during volitional movement. Despite subject-specific spectral profiles, a consistent finding across patients was that oscillatory power was strongest and had the largest magnitude of modulation during movement in LFPs recorded from segments facing the postero-lateral "sensorimotor" region of GPi, whereas antero-medially-directed segmented contacts facing the internal capsule and/or anterior GPi, had relatively weaker LFP power and less modulation in the 5 to 35 Hz. In each subject, contact configurations chosen for clinically therapeutic stimulation (following data collection and blinded to physiology recordings), were in concordance with the contact pairs showing the largest amplitude of LFP oscillations in the 5-35 Hz range. Although limited to three subjects, these findings provide support for the hypothesis that the sensorimotor territory of the GPi corresponds to the site of maximal power of oscillatory activity in the 5 to 35 Hz and provides the greatest benefit in motor signs during stimulation in the GPi. Variability in oscillatory activity across patients is likely related to Parkinson's disease phenotype as well as small differences in recording location (i.e. lead location), highlighting the importance of lead location for optimizing stimulation efficacy. These data also provide compelling evidence for the use of LFP activity for the development of predictive stimulation models that may optimize patient benefits while reducing clinic time needed for programming.

Keywords

GPi; segmented; DBS; local field potential; Parkinson's disease

Introduction

Parkinson's disease is a neurodegenerative disease for which deep brain stimulation (DBS) is an effective therapy for treating motor signs. Neurophysiological data collected from (temporary) microelectrodes and (implanted) DBS lead contacts have led to ground breaking work in understanding the pathophysiology of Parkinson's disease. Local field potential (LFP) recordings from recently introduced directional (segmented) deep brain stimulation (dDBS) leads may provide even further insights into the pathophysiology of Parkinson's disease and be a useful tool to inform programming strategies that optimize clinical benefit. Previous studies in the subthalamic nucleus (STN) using omnidirectional ring electrodes for recording LFPs reported the most beneficial effect of STN DBS arose from those contacts with the highest magnitude of beta activity (Ince et al., 2010; Yoshida et al., 2010). Similarly, a subsequent report suggested that the site of beta activity with the greatest relative power determined through DBS lead recordings could reasonably predict the site within the STN for optimal outcomes (Horn et al., 2017). Data from these studies suggest that LFP recordings from DBS electrodes have the potential to guide patient programming and identify the optimal locations within the DBS target for implantation. The recent development of dDBS leads with segmented (i.e. directional) contacts offers higher spatial resolution when recording LFP activity compared to omnidirectional contacts and enables us to better define the spatial distribution of biomarker activity and determine whether this

activity might be predictive of which segments provide optimal clinical efficacy (Tinkhauser et al., 2018).

Despite the fact that the internal segment of the globus pallidus (GPi) is increasingly being targeted for DBS in Parkinson's disease patients, there are few reports exploring the presence and spatial distribution of LFP activity in the pallidum (AuYong et al., 2018; Silberstein et al., 2003; Tsiokos et al., 2013), none of which include dDBS leads. The goal of the present study was to identify the spectral characteristics, spatial topography, and movement-related dynamics of LFP activity in the GPi in patients with Parkinson's disease with externalized dDBS leads. These data serve as a step towards characterizing electrophysiological biomarkers in the pallidum, improving our understanding of the pathophysiological basis underlying Parkinson's disease motor signs and providing insights that could inform DBS programming, thereby enhancing clinical efficacy and minimize programming time. These data will also serve as the basis for successfully implementing electrophysiological biomarker-based closed-loop stimulation applications for patients receiving GPi DBS with directional leads.

Materials and methods

Subjects

All procedures were approved by the University of Minnesota Institutional Review Board (#1701M04144) and subjects' consent was obtained according to the Declaration of Helsinki. Three patients (two females, one male) with idiopathic Parkinson's disease approved for DBS by our DBS consensus committee were consented for externalization and enrolled in the study. The University of Minnesota DBS consensus committee determines surgical candidacy and target selection through a standard of care, multi-disciplinary patient review process that involves Neurology, Neurosurgery, Neuropsychology and Nursing. General criteria for candidacy include (but not limited to): diagnosis of idiopathic Parkinson's disease by a movement disorders neurologist, minimum of five years disease duration, significant disability despite medical management, nondemented, equal to or greater than 30% increase in the Unified Parkinson's Disease Rating Scale (UPDRS)-III (motor subsection) scores with levodopa treatment compared to off mediation (except when treating refractory tremor), adequate post-surgery social support, no major and/or uncontrolled psychiatric or medical disease. The review process and subsequent surgical procedure is standard of care and was independent of the patient's participation in this study. Demographics and phenotypic characteristics for each patient are provided in Table 1.

GPi DBS Implantation and Externalization Procedure

Prior to surgery, patients underwent a standard 3T MRI. A high resolution 7T MRI was also obtained, primarily for postoperative lead localization (see "Image-Based Reconstruction of DBS Lead Location and Orientation" below). Standard 3T images were imported into a Stealth neuronavigation system (Medtronic, Inc., Dublin, Ireland) for direct targeting and trajectory planning. Also imported into the Stealth system was 3T MR imaging containing highlighted GP borders, which were determined using the 7T MR imaging, to identify pallidal borders and directly target the posterolateral region of the GPi (Duchin et al., 2018,

2012; Patriat et al., 2018). On the morning of surgery, a CT of the head was obtained with the stereotactic frame fixed to the skull. The CT was then imported into the Stealth system and merged with preoperative imaging and planned trajectory. Intraoperative electrophysiological mapping techniques (Vitek et al., 1998) were used to confirm the location of the intended implant site. The planned trajectories of microelectrodes used for mapping, and subsequent lead placements, were anterior to posterior (range: 58.5° - 62.3° from horizontal) and slightly lateral to medial (range: 1.5° - 4.4° from vertical). A segmented "1-3-3-1" electrode (Abbott St. Jude Medical model 6172, contact height: 1.5 mm with 0.5 mm vertical spacing) was then implanted in the sensorimotor region of GPi. After lead implantation, tunneling was performed from the mastoid region to a subcutaneous pocket superficial to the pectoralis muscle in the infraclavicular region where a lead extension (Abbott St. Jude Medical model 6372) was placed and connected to the proximal end of the DBS lead. Rather than connecting the lead extension to an implantable pulse generator (IPG), the distal end of the DBS lead extension was connected to a "percutaneous" extension (Abbott St. Jude Medical Model 3383)) within the infraclavicular pocket and then tunneled from the inferior aspect of the pocket to the ipsilateral superior quadrant of the abdominal area where it was externalized, leaving a 3 cm segment protruding outside the abdominal pocket. The externalized segment was connected to the Abbott St. Jude Medical Multilead Trial Cable (model 3014) to enable subsequent connections to our electrophysiology recording equipment. The externalized components were secured and protected with a waterproof barrier dressing (Tegaderm, 3M, Maplewood, MN). Subjects were discharged to home until externalization recordings, which occurred 4-7 days after implantation. This approach allowed time for patients to recover after the lead implantation procedure and helped mitigate confounds related to temporary motor sign improvement immediately following lead placement (Koop et al., 2006).

Study protocol

Participants were admitted to the University of Minnesota Health Clinical Research Unit where spontaneous and task-related LFP activity was recorded from the DBS lead over the course of 48 hours. Electroencephalogram (EEG) data collected as part of the protocol is not reported here. The distal end of the trialing cable was connected to an ATLAS Neurophysiological System (NeuraLynx, Inc., Bozeman, MT) via an adapter cable (FHC, Inc., Bowdoin, ME). Neural data were acquired (EEG scalp contacts used for reference and ground) and digitized at 24kHz for subsequent analysis. Electromyographic (EMG) and kinematic activity from the contralateral upper extremity were recorded simultaneously with LFP recordings, using Delsys Trigno Legacy EMG and inertial measurement unit (IMU) wireless sensors (Delsys, Inc., Natick, MA).

All data presented here were collected after overnight withdrawal of parkinsonian medication, with the patient sitting in a hospital bed in a standard Fowler position. Data were collected in two behavioral conditions: rest and goal-oriented reaching. ***Rest:*** subjects were instructed to look at a predetermined point on the wall and remain still with their eyes open for five minutes. ***Reach task:*** subjects placed the hand contralateral to the implanted DBS lead (e.g. left GPi lead, right hand used) on a digitized home button, which was located 45 cm (Euclidean distance) from the target location displayed on a touchscreen monitor.

After a randomized variable 3-5 sec delay following the start of a trial, a 1.27 cm hollow circle (initial target) appeared on the center of the touchscreen along with a 5 cm square box (final target) directly to the left of the circle. The distance between the initial (circle) and the final (square) targets was 10 cm, center to center. The appearance of the circle and square was the patient's "go cue". Subjects were instructed to touch and drag the circle into the square box as quickly and accurately as possible and then return to the home button (50 total trials). Initiating a movement prior to the go cue, or failing to reach the target within a 10 s window resulted in the trial being removed from further offline analysis. See the online supplemental video of a subject completing the reach task.

At the conclusion of the 2-day externalization study, subjects returned to the hospital for removal of the percutaneous extension and placement of the IPG. Subjects returned to the Neurology clinic approximately 4-6 weeks after IPG placement for their initial DBS programming, per standard clinical care. The movement disorders clinician performing the DBS programming was still blinded to the physiological recordings and was instructed to select programming parameters per their routine standard of care.

Local Field Potential Analysis

All analyses were performed using customized scripts in MATLAB (MathWorks, 2016). The Abbott St. Jude Medical 8-channel directional lead (model 6172) is constructed in a "1-3-3-1" fashion (totaling 8 contacts). For the purposes of description in this manuscript, we use the term "contact" to refer to any of the eight single electrodes (i.e. contact point through which data was recording or stimulation could be delivered), we use the term "ring" to refer to a vertical level of contact(s) (e.g. ring 1 has one contact, ring 2 has three contacts, etc.) and we use the word "segment" to refer to individual contacts of the segmented rings 2 and 3 (i.e. 2a,b,c; 3a,b,c). See Fig. 1A. Each contact of ring 2 and 3 ("a", "b" and "c") have a surface area of 1.8 mm^2 and ring 1 and 4 have a surface area of 6.2 mm^2. Just dorsal to the fourth ring is a radial marker, with a fiducial aligned vertically with contacts 2a and 3a, for the purpose of orienting the lead. Total diameter of the lead is 1.27 mm. LFPs from the pallidum were constructed from bipolar pairs of contacts by subtracting recordings from vertically adjacent contacts of the DBS leads. Between segmented rings 2 and 3, vertical aligned contacts were used to construct LFPs (e.g. 2a-3a represents the signal created by subtracting the signal of contact 3a from 2a). For signal between segmented and non-segmented rings, we constructed bipolar pairs between each contact of the segmented rings with the adjacent continuous ring (e.g. 3a-4 represents the signal created by subtracting the signal of contact 4 from 3a). Additionally, for the purpose of comparing LFP recordings of dDBS leads with non-directional DBS leads, virtual ring recordings for the segmented rows, rings 2 and 3, were generated by averaging all contacts of ring 2 (a, b and c) and all contacts of ring 3 (a, b and c), respectively. In subject 3, ring 1 contained cardiac artifacts that were attenuated using a template subtraction technique. Changes in oscillatory power over time were visualized using spectrograms computed with the *spectrogram* function using 2^{16} points in the discrete Fourier transform, a Hamming window of 2^{14} points and 50% overlap. The frequency resolution was 0.3662 Hz. Power spectral density (PSD) plots were generated from spectrograms calculated over 5 minutes of continuous recordings in the rest condition.

Spectrograms were divided into 15-second epochs, averaged over time, resulting in 20 PSD traces.

The effects of movement on oscillatory activity in the GPi were evaluated using the following methods: First, spectrograms of LFP data collected during the reach task were computed via the multi-taper method and Chronux toolbox (Bokil et al., 2010) with a frequency resolution of ~1 Hz and time resolution of 25 ms. For each trial, the time point of maximal hand angular velocity during the reach to target was identified based on the Delsys gyroscope signals. A 'reach' PSD was generated for each trial by averaging the spectrogram in a 200 ms window centered on the time point of maximum velocity of their reach within each trial. Similarly, 'pre-movement' PSDs were generated for each trial by averaging the spectrogram in a 200ms window 1.5 seconds prior to reach initiation while the patient's hand was resting on the start pad. The statistical significance of differences in median spectral power between 'pre-movement' and 'reach' PSDs was assessed using the Wilcox on rank sum (WRS) test ($p = 0.01$) at each frequency bin in the PSD, with Bonferroni correction for the number of frequency bins in the 3-40 Hz frequency range of interest (n=37). Two consecutive bins had to pass the WRS-test for a difference to be considered significant.

Image-Based Reconstruction of DBS Lead Location and Orientation

High-resolution 7T MR images (T2-weighted 0.4x0.4x1mm) were acquired prior to surgery for each patient and borders of the GPi and globus pallidus extemus (GPe) were manually segmented (Duchin et al., 2012, 2018; Patriat et al., 2018). Tractography-based parcellation (diffusion weighted 1.5x1.5x1.5mm) of the GPi was performed in subject 3 in order to provide an example of sub-regions of GPi (for further details including image acquisition parameters and processing steps, see (Patriat et al., 2018) (see axial images in Fig. 1D). Approximately one month following IPG placement, high-resolution CT images (0.4x0.4x0.6mm) were acquired to visualize the DBS lead. This 1-month CT image was then registered with the preoperative 7T MR image using a rigid, followed by an affine, transformation within 3D Slicer (http://www.slicer.org, (Fedorov et al., 2012)). A 3D model was created depicting the DBS lead location and its axial orientation, with respect to the patient-specific pallidum segmentation (Fig. 1, left panels). The orientation of the DBS lead and relative direction of individual segments (a, b and c) for each patient were derived from the fiducial marker directly superior to contact 4, in combination with the unique artifact characteristics of the segments, using a modified version of the DiODe algorithm (Hellerbach et al., 2018) and confirmed with information extracted from fluoroscopy and X-ray images acquired intraoperatively.

Data Availability

The data that support the findings in this study are available from the corresponding author, JV, upon reasonable request.

Results

Three-dimensional reconstructions of the location of each contact, for each patient, is represented in Fig. 1B, C and D, showing orientation and trajectory of the lead across three different views of the pallidum (sagittal, coronal, axial). Directly to the right of the 3D images are axial cross-sectional views of the pallidum depicting the location and orientation of the segmented contacts of rings 2 and 3. Although in slightly different locations of the pallidum, all three leads are in the sensorimotor region of the GPi as confirmed by intraoperative microelectrode recordings during which proprioceptive fields were observed. Relative to each other's lead location within the sensorimotor territory, subject 1's lead is located in a slightly more anterior and medial area of the sensorimotor territory, subject 2's lead location is more posterior and lateral, while subject 3's lead location is posterior and medial.

Spectrograms are shown in Fig. 1B for vertically aligned rings and segments (from left to right) 'b', 'a' and 'c' (aligned to the orientation of the lead – Fig. 1A). The far-right panel of Fig. 1B shows recordings for virtual rings, as described in the methods. For all subjects, when segmented contacts of the same ring were averaged to simulate a single, uniform ring recording, maximum power of LFP activity was reduced compared to segmented contact recordings. All three subjects had spatially distinct oscillatory activity across 'a', 'b' and 'c' segment directions, as well as unique spectral profiles as described in the following section. Power spectral densities (2-350 Hz) for directional LFPs from vertically-aligned segment pairs (from rings 2 and 3) for all three subjects are shown in Fig. 2 (mean +/− 2SD). Described here are oscillations and/or modulation of frequencies ≤35 Hz. High frequency oscillations in the 200-250Hz range observed in all three patients are not described in detail in this manuscript (See Fig. 2).

The DBS montage selected in clinic during the patient's initial programming visit for providing therapeutic stimulation is shown for each patient, in red on the two-dimensional MRI images and also written in red italics underneath the third column (segment 'c') of the LFP spectrograms (Fig. 1). Stimulation through individual segmented contacts was not attempted in subject 2 during the initial programming session (monopolar review). For all three patients, the clinician performing the monopolar review was not given programming constraints and was told to program the patient per their normal standard of care protocol.

LFPs at Rest

Spectral features described below were most prominent in LFPs recorded from segments facing the postero-lateral "sensorimotor" region of GPi, whereas medial or medial-anterior facing segments displayed, overall, oscillatory power that was relatively lower in amplitude (See Fig. 1). Subject 1 had a prominent theta-range 7 Hz peak that was highest in amplitude within the 2c-3c (posterior facing) segment pair (Fig. 1B). A smaller low beta 13 Hz peak was also present and found predominantly in contact pairs 2a-3a, 2c-3c, to a relatively lesser extent in 1-2c and trace amounts in the remaining contact pairs. Phenotypically, this subject displayed predominantly lower extremity rest tremor and to a lesser extent, upper extremity rest tremor, as well as upper and lower extremity rigidity and bradykinesia. Subject 2 had a prominent high beta 29 Hz peak with the largest amplitude found in the 2b-3b (postero-

lateral facing) segment pair (Fig. 1C). Phenotypically this subject had minimal tremor but moderate rigidity with marked bradykinesia and postural and gait instability. Subject 3 displayed double-peak oscillatory power at 20 Hz and 29 Hz with a broader distribution across multiple segments, but greatest in the direction of segments a and b (Fig. 1D) that were facing the posterior and lateral regions of sensorimotor GPi. This subject displayed tremor in the upper limbs, rigidity, and bradykinesia. The most significant feature to this patient's symptomatology, however, was his gait disorder manifesting predominantly as freezing of gait.

LFPs During a Reach Task

Fig. 3 shows spectrograms over 60 seconds during rest and the reach task (approximately 8-10 reaches) for each subject and represents vertically-aligned differential recordings from the segmented contacts (2a-3a, 2b-3b, 2c-3c). These plots illustrate oscillatory activity in subject-specific contact pairs, demonstrating task-related modulation in oscillations that are location-specific within the pallidum.

Subject 1 displayed a prominent low frequency peak in the range of 5-10 Hz, and in the low beta 12-15 Hz range just prior to reaching, with power greatest in the direction of segments 2c-3c (facing the posterior region of GPi). A non-significant ($p > 0.01$) modulation (reduction) in power across both theta and low beta was elicited during the reach task relative to the premovement time period (the time period between reach trials when the subject's arm was in the rest position) (Fig. 4A). Noteworthy is the location of rings 2 and 3 in the axial view (Fig. 1) within the GPi for this subject, which may be mesial relative to reported "arm/hand" somatotopic regions of GPi (Baker et al., 2010; Vitek et al., 1999) and, therefore, could underlie the minimal modulation in oscillatory activity observed during the reach-task (see Fig. 3A and 4A).

Subject 2. In bipolar recordings from segments of the ring pair 2-3, subject 2 exhibited a significant reduction in high beta power (around 30 Hz) during reaching compared to rest, while low frequency oscillatory activity was significantly increased during movement ($p < 0.01$) (Fig. 3B and 4B). Reductions in high beta frequency oscillations during movement were most evident on contact 'b' (postero-lateral facing) (Fig. 3B), the same contact pair where high beta was greatest during the rest condition, while the increase in low frequency oscillatory activity was greatest in the direction of contacts 'a' (anterior facing) and 'c' (medial facing). During movement we observed a single peak frequency at around 25 Hz in all directional contacts ('a', 'b' and 'c') (Fig. 4B).

Subject 3. In bipolar recordings from the segments of ring pair 2-3, modulation in the beta frequencies was most evident in the direction of contacts 'a' (antero-lateral) and 'b' (postero-lateral), where power was significantly reduced during reach, as compared to rest, in the 10-20 Hz and 25-35 Hz ranges ($p < 0.01$) (Fig. 4C). It is noteworthy that in this subject, broad band activity was apparent across multiple contact pairs (Fig. 1D). Similar to subject 2, low frequency (2-11 Hz) oscillatory activity was significantly increased during movement ($p < 0.01$) compared to pre-movement rest phases and this, like subject 2, occurred in contact pairs that showed the lowest amount of modulation in the beta frequencies. For subject 3, this was in the direction of contact 'c', which was also antero-

medial facing, as was contact ‘a’ and ‘c’ for subject 2. Also similar to subject 2, during movement we observed a single peak frequency at around 25 Hz in all directional contacts (‘a’, ‘b’ and ‘c’). Videos of subject 3 performing the reach task, time-aligned to oscillatory activity measured from the DBS leads, are available in the Supplementary Materials.

Discussion

Physiological biomarkers are subject-specific and spatially localized within the GPi

Although multiple studies have recorded LFP activity from the STN in patients with Parkinson’s disease, there are few reports of this activity in the pallidum. In three Parkinson’s disease patients with recently implanted dDBS leads in the GPi we observed the presence of LFP activity in multiple frequency bands that were present at rest and were modulated during a goal-orientated reaching movement. This patient-specific LFP activity was spatially selective (i.e. differentially present in adjacent segments of the same ring) with power greatest in the segments that were predominately facing the posterolateral “sensorimotor” portions of GPi. When segments were computed as a virtual ring, power of LFP activity in the “ring mode” was reduced compared to that found in selective segments of the corresponding rings, suggesting that recordings from omnidirectional rings may average out spatially selective biomarker activity. While sensing in the ring mode can reveal the presence of and changes in LFP activity under different conditions, segmented leads can provide a more regionally-specific view of such activity and relative power in different regions of GPi. Inter- and intra-subject variability in principal frequency content from LFP activity could be a function of one or multiple factors, which may include: recording from omnidirectional rings (washing out specific regions of oscillations), recording in differing regions within a nucleus containing phenotype-specific physiological activity or differing regions containing somatotopy-specific physiological activity. Notably, further washout can occur when averaging across patients. Thus, given the specificity of the spatial distribution of biomarker activity in GPi along with the range of peak frequency oscillations that we observed in these three patients, one should also be cautious when interpreting the absence/presence of LFP activity, or its relationship to specific motor signs, particularly when averaged across Parkinson’s disease patients with different phenotypic profiles and whose leads may be in relatively different regions of the targeted area.

Lead location relative to anatomical structures: Implications for lead placement and DBS programming

Earlier studies using omnidirectional ring electrodes for recording LFPs reported that the most beneficial effect of STN DBS arose from those contacts with the highest magnitude of beta activity (Ince et al., 2010; Yoshida et al., 2010). Similar to findings reported for the STN (Horn et al., 2017; Tinkhauser et al., 2018), the clinically chosen contact(s) for therapeutic stimulation in our three subjects align well with the contact pairs in the sensorimotor region of GPi showing the greatest power of oscillatory activity. Thus, the DBS lead orientation and directional LFP recordings presented here may lead to better outcomes by allowing more spatially precise LFP-guided DBS programming, which is dependent on lead location, in particular, targeting the sensorimotor portion of GPi.

In next steps, we are utilizing precise localization of each directional contact within the GPi (as reported here), and developing three-dimensional probabilistic maps of LFP activity in GPi and examining their relationship to phenotype and clinical outcomes with stimulation in these different pallidal regions. Once collected in a larger cohort of patients these data would allow us to identify the optimal target location within the structure for lead placement, which may prove to vary slightly depending on patient phenotype. This then sets the stage for developing automated algorithms that can predict optimal stimulation parameters based on phenotype and location of the lead, potentially reducing the time and expertise needed in the clinic for programming or even enable telemedicine-based programming.

Oscillatory activity in the GPi in Parkinson's disease: Relationship to motor signs

Even in this small patient cohort, we observe differing oscillatory activity patterns between subjects, which may be related to patient phenotype or recording location or a combination of both. For example, subject 1, who presented with tremor in both upper and lower limbs along with bradykinesia, demonstrated two spectral peaks, one previously reported to be relevant to the presence of tremor (theta) and the other to bradykinesia (low beta) (Brown, 2003; Kühn et al., 2009). This spectral activity was most prominent in segments facing posterior and lateral regions of GPi. Subject 2, who presented with bradykinesia, rigidity and gait problems, showed predominately high beta oscillatory power; while subject 3, who had marked midline/axial-related signs including gait disturbance and prominent freezing along with bradykinesia and rigidity, displayed broad spectrum oscillatory activity across a wide range of contacts with a noticeable double peak, one in low and one in high beta frequency ranges. Similar to subject 1, oscillations with the largest amplitude were, in general, facing the posterior and lateral region of GPi in both subject 2 and 3. Interestingly, both subject 2 and subject 3 showed a single peak oscillation around 25 Hz during goal-orientated reaching, which was a shift from frequency peak(s) noted during the premovement rest phase. Although peak oscillations during the premovement rest phase (Fig. 4) were similar to those recorded during a true rest condition (Fig. 2), consideration should be given to the potential for anticipatory-induced modulation just prior to movement (Hendrix et al., 2018).

With respect to utilizing physiological activity for determining clinical DBS programming, a single segmented contact was clinically chosen for therapeutic stimulation (3b-, case+) for subject 3. Given the spatially broad range of oscillatory activity, one could theorize that, for this patient, stimulating a greater volume of GPi by creating a larger volume of activation via stimulation through multiple contacts at lower currents could potentially result in improved outcomes or a larger therapeutic window. It is also possible that phenotype-specific frequency oscillations (which may or may not be spatially distinct) should be targeted and stimulating spatially different contacts, independently, could be used to target specific frequencies where they are identified to be most prominent. Clearly a limitation here is the number of patients and, therefore, a larger number of patients will be required to evaluate the predictive power of biomarker detection from dDBS pallidal LFPs, for both characterizing the relationship of LFP activity to individual motor signs and determining the optimal contact(s) for dDBS. As our knowledge of underlying physiological processes becomes better defined, mapping the physiological features onto specific sub-regions of each DBS

target will be a critical step in tailoring stimulation location and parameters to specific disease features of individual patients.

Implications for closed-loop deep brain stimulation in the GPi

Next generation DBS devices may incorporate real-time measures of LFP activity to inform how stimulation is delivered. Indeed, several studies have suggested therapeutic benefit to adjusting stimulation parameters based on the presence and power of beta oscillations in the STN (Little et al., 2016a, 2016b, 2013; Priori et al., 2013; Rosa et al., 2017, 2015). Our findings highlight several important considerations for LFP-based closed-loop DBS. First, our data shows that oscillatory activity in GPi dynamically changes during volitional movement. This is noteworthy because the frequencies currently being targeted as biomarkers for implementing closed-loop algorithms, such as beta frequencies, do indeed modulate during volitional movement, and these dynamic changes in biomarker activity can result in corresponding changes in stimulation that negatively impact the efficacy of closed-loop (Johnson et al., 2016). Second, algorithms will need to consider each individual's unique spectral and spatial topography of oscillatory activity (i.e. which frequencies are important and from which direction are they coming). Equally important then, will be knowledge of the precise location of the lead, which may influence modulation of oscillatory activity that is captured during both volitional movement and at rest. The relationship between "normal" resting state oscillations and modulation from volitional movement and the changes in this relationship that occur with the development of Parkinson's disease requires further elucidation but will most certainly need to be accounted for in future closed-loop algorithms.

Summary

Externalized recordings from three Parkinson's disease patients using directional DBS leads revealed a spatial topography of oscillatory activity in the pallidum, demonstrated spectral characteristics, in particular, frequency bands and peaks, that were distinct for each patient, and showed modulation of these characteristics with volitional movement. Although the peak frequency of oscillatory activity varied across patients, maximum power was always found in segments that faced the posterolateral "sensorimotor" territory of GPi and aligned with the clinically chosen contacts. This study demonstrates the utility of using patient-specific data for determining the relative location and orientation of the individual lead contacts for characterizing the relationship of LFP activity to individual motor signs and potentially determining the optimal contact(s) for DBS. Oscillatory activity modulated with movement, emphasizing the context dependent nature of these biomarkers that will need to be accounted for in order to improve efficiency and for providing patient-specific DBS therapy, such as closed-loop DBS. Whether causal or epiphenomenal, the ability to define the roles of patho- and non-pathophysiological oscillatory activity in Parkinson's disease has significant implications for optimizing closed-loop algorithms. Still, although the functional meaning of these oscillations has not yet been fully elucidated, the fact they are spatially distributed in different regions of GPi, and are patient-specific, further emphasizes the importance of lead location in determining clinical outcomes. As our knowledge of underlying physiological processes becomes better defined, mapping the physiological

features onto specific sub-regions of each DBS target will be a critical first step in tailoring stimulation location and parameters to specific disease features of individual patients.

Supplementary Material

Refer to Web version on PubMed Central for supplementary material.

Acknowledgements

We would like to acknowledge the following people for their contributions to this study: Greg Molnar for his help with acquiring equipment components and for helpful insights regarding sensing with directional DBS leads; Sommer Huffmaster for suggestions regarding data collection; the entire UMN Udall team for critiques and comments on the manuscript.

Funding

This work was supported by the Udall Center for Excellence in Parkinson's Disease, National Institutes of Health - National Institute of Neurological Disorders and Stroke: P50-NS098573, R01-NS081118, R01-NS113746, P30-NS076408, P41-EB027061; MnDRIVE (Minnesota's Discovery, Research and Innovation Economy) Brain Conditions Program; Engdahl Family Foundation; The Kurt B. Seydow Dystonia Foundation; Parkinson Study Group; and the Parkinson's Disease Foundation's Advancing Parkinson's Treatments Innovations Grant

Declaration of Interests and Financial Disclosures

Noam Harel - consultant and a shareholder for Surgical Information Sciences Inc. **Remi Patriat** - consultant for Surgical Information Sciences Inc. **Michael Park** - Listed faculty for University of Minnesota Educational Partnership with Medtronic, Inc., Minneapolis, MN, Consultant for: Zimmer Biomet, Synerfues, Inc, NeuroOne, Boston Scientific. Grant/Research support from: Medtronic, Inc., Boston Scientific, Abbott. **Jerrold Vitek** - Consultant for: Medtronic, Inc., Boston Scientific, Abbott, Surgical Information Sciences, Inc.

Abbreviations:

dDBS	directional deep brain stimulation
T	tesla
IMU	inertial measurement unit

References

AuYong N, Malekmohammadi M, Ricks-Oddie J, Pouratian N, 2018 Movement-Modulation of Local Power and Phase Amplitude Coupling in Bilateral Globus Pallidus Interna in Parkinson Disease. Front. Hum. Neurosci 12 10.3389/fnhum.2018.00270

Baker KB, Lee JYK, Mavinkurve G, Russo GS, Walter B, DeLong MR, Bakay RAE, Vitek JL, 2010 Somatotopic organization in the internal segment of the globus pallidus in Parkinson's disease. Exp. Neurol 222, 219–225. 10.1016/j.expneurol.2009.12.030 [PubMed: 20059997]

Bokil H, Andrews P, Kulkarni JE, Mehta S, Mitra PP, 2010 Chronux: A platform for analyzing neural signals. J. Neurosci. Methods 192, 146–151. 10.1016/j.jneumeth.2010.06.020 [PubMed: 20637804]

Brown P, 2003 Oscillatory nature of human basal ganglia activity: relationship to the pathophysiology of Parkinson's disease. Mov. Disord. Off. J. Mov. Disord. Soc 18, 357–363. 10.1002/mds.10358

Duchin Y, Abosch A, Yacoub E, Sapiro G, Harel N, 2012 Feasibility of Using Ultra-High Field (7 T) MRI for Clinical Surgical Targeting. PLOS ONE 7, e37328 10.1371/journal.pone.0037328 [PubMed: 22615980]

Duchin Y, Shamir RR, Patriat R, Kim J, Vitek JL, Sapiro G, Harel N, 2018 Patient-specific anatomical model for deep brain stimulation based on 7 Tesla MRI. PLOS ONE 13, e0201469 10.1371/journal.pone.0201469 [PubMed: 30133472]

Fedorov A, Beichel R, Kalpathy-Cramer J, Finet J, Fillion-Robin J-C, Pujol S, Bauer C, Jennings D, Fennessy F, Sonka M, Buatti J, Aylward S, Miller JV, Pieper S, Kikinis R, 2012 3D Slicer as an Image Computing Platform for the Quantitative Imaging Network. Magn. Reson. Imaging 30, 1323–1341. 10.1016/j.mri.2012.05.001 [PubMed: 22770690]

Hellerbach A, Dembek TA, Hoevels M, Holz JA, Gierich A, Luyken K, Barbe MT, Wirths J, Visser-Vandewalle V, Treuer H, 2018 Directional Orientation Detection of Segmented Deep Brain Stimulation Leads: A Sequential Algorithm Based on CT Imaging. Stereotact. Funct. Neurosurg 96, 335–341. 10.1159/000494738

Hendrix CM, Campbell BA, Tittle BJ, Johnson LA, Baker KB, Johnson MD, Molnar GF, Vitek JL, 2018 Predictive encoding of motor behavior in the supplementary motor area is disrupted in parkinsonism. J. Neurophysiol 120,1247–1255. 10.1152/jn.00306.2018 [PubMed: 29873615]

Horn A, Neumann W-J, Degen K, Schneider G-H, Kühn AA, 2017 Toward an electrophysiological "sweet spot" for deep brain stimulation in the subthalamic nucleus. Hum. Brain Mapp 38, 3377–3390. 10.1002/hbm.23594 [PubMed: 28390148]

Ince NF, Gupte A, Wichmann T, Ashe J, Henry T, Bebler M, Eberly L, Abosch A, 2010 Selection of Optimal Programming Contacts Based on Local Field Potential Recordings From Subthalamic Nucleus in Patients With Parkinson's Disease. Neurosurgery 67, 390–397. 10.1227/01.NEU.0000372091.64824.63 [PubMed: 20644424]

Johnson LA, Nebeck SD, Muralidharan A, Johnson MD, Baker KB, Vitek JL, 2016 Closed-loop deep brain stimulation effects on parkinsonian motor symptoms in a non-human primate -- is beta enough? Brain Stimulat 9, 892–896. 10.1016/j.brs.2016.06.051

Koop MM, Andrzejewski A, Hill BC, Heit G, Bronte-Stewart HM, 2006 Improvement in a quantitative measure of bradykinesia after microelectrode recording in patients with Parkinson's disease during deep brain stimulation surgery. Mov. Disord 21,673–678. 10.1002/mds.20796 [PubMed: 16440333]

Kühn AA, Tsui A, Aziz T, Ray N, Brücke C, Kupsch A, Schneider G-H, Brown P, 2009 Pathological synchronisation in the subthalamic nucleus of patients with Parkinson's disease relates to both bradykinesia and rigidity. Exp. Neurol 215, 380–387. 10.1016/j.expneurol.2008.11.008 [PubMed: 19070616]

Little S, Beudel M, Zrinzo L, Foltynie T, Limousin P, Hariz M, Neal S, Cheeran B, Cagnan H, Gratwicke J, Aziz TZ, Pogosyan A, Brown P, 2016a Bilateral adaptive deep brain stimulation is effective in Parkinson's disease. J. Neurol. Neurosurg. Psychiatry 87, 717–721. 10.1136/jnnp-2015-310972 [PubMed: 26424898]

Little S, Pogosyan A, Neal S, Zavala B, Zrinzo L, Hariz M, Foltynie T, Limousin P, Ashkan K, FitzGerald J, Green AL, Aziz TZ, Brown P, 2013 Adaptive Deep Brain Stimulation In Advanced Parkinson Disease. Ann. Neurol 74, 449–457. https://doi.org/10.1002/ana.23951 [PubMed: 23852650]

Little S, Tripoliti E, Beudel M, Pogosyan A, Cagnan H, Herz D, Bestmann S, Aziz T, Cheeran B, Zrinzo L, Hariz M, Hyam J, Limousin P, Foltynie T, Brown P, 2016b Adaptive deep brain stimulation for Parkinson's disease demonstrates reduced speech side effects compared to conventional stimulation in the acute setting. J. Neurol. Neurosurg. Psychiatry 87, 1388–1389. 10.1136/jnnp-2016-313518 [PubMed: 27530809]

Patriat R, Cooper SE, Duchin Y, Niederer J, Lenglet C, Aman J, Park MC, Vitek JL, Harel N, 2018 Individualized tractography-based parcellation of the globus pallidus pars interna using 7T MRI in movement disorder patients prior to DBS surgery. NeuroImage 178, 198–209. 10.1016/j.neuroimage.2018.05.048 [PubMed: 29787868]

Priori A, Foffani G, Rossi L, Marceglia S, 2013 Adaptive deep brain stimulation (aDBS) controlled by local field potential oscillations. Exp. Neurol., Special Issue: Neuronal oscillations in movement disorders 245, 77–86. 10.1016/j.expneurol.2012.09.013

Rosa M, Arlotti M, Ardolino G, Cogiamanian F, Marceglia S, Fonzo AD,Cortese F, Rampini PM, Priori A, 2015 Adaptive deep brain stimulation in a freely moving parkinsonian patient. Mov. Disord 30, 1003–1005. 10.1002/mds.26241 [PubMed: 25999288]

Rosa M, Scelzo E, Locatelli M, Carrabba G, Levi V, Arlotti M, Barbieri S, Rampini P, Priori A, 2017 Risk of Infection After Local Field Potential Recording from Externalized Deep Brain Stimulation

Leads in Parkinson's Disease. World Neurosurg. 97, 64–69. 10.1016/j.wneu.2016.09.069 [PubMed: 27686508]

Silberstein P, Kühn AA, Kupsch A, Trottenberg T, Krauss JK, Wöhrle JC, Mazzone P, Insola A, Di Lazzaro V, Oliviero A, Aziz T, Brown P, 2003 Patterning of globus pallidus local field potentials differs between Parkinson's disease and dystonia. Brain 126, 2597–2608. 10.1093/brain/awg267 [PubMed: 12937079]

Tinkhauser G, Pogosyan A, Debove I, Nowacki A, Shah SA, Seidel K, Tan H, Brittain J-S, Petermann K, di Biase L, Oertel M, Pollo C, Brown P, Schuepbach M, 2018 Directional Local Field Potentials: A Tool to Optimize Deep Brain Stimulation. Mov. Disord 33, 159–164. [PubMed: 29150884]

Tsiokos C, Hu X, Pouratian N, 2013 200–300Hz movement modulated oscillations in the internal globus pallidus of patients with Parkinson's Disease. Neurobiol. Dis 54, 464–474. 10.1016/j.nbd.2013.01.020 [PubMed: 23388190]

Vitek JL, Bakay RAE, Hashimoto T, Kaneoke Y, Mewes K, Zhang JY, Rye D, Starr P, Baron M, Turner R, Delong MR, 1998 Microelectrode-guided pallidotomy: technical approach and its application in medically intractable Parkinson's disease. Spec. Suppl 113, 1027–1043. 10.3171/jns.1998.88.6.1027@sup.2010.113.issue-3

Vitek JL, Chockkan V, Zhang J-Y, Kaneoke Y, Evatt M, DeLong MR, Triche S, Mewes K, Hashimoto T, Bakay RAE, 1999 Neuronal activity in the basal ganglia in patients with generalized dystonia and hemiballismus. Ann. Neurol 46, 22–35. 10.1002/1531-8249(199907)46:1<22::AID-ANA6>3.0.CO;2-Z [PubMed: 10401777]

Yoshida F, Martinez-Torres I, Pogosyan A, Holl E, Petersen E, Chen CC, Foltynie T, Limousin P, Zrinzo LU, Hariz MI, Brown P, 2010 Value of subthalamic nucleus local field potentials recordings in predicting stimulation parameters for deep brain stimulation in Parkinson's disease. J. Neurol. Neurosurg. Psychiatry 81, 885–889. 10.1136/jnnp.2009.190918 [PubMed: 20466699]

Highlights

- Recordings from directional deep brain stimulation leads in Parkinson's disease.
- Patient-specific 7-Tesla MRI for reconstructing individual lead contact locations.
- Spatially-localized oscillatory activity within the globus pallidus internus.
- Patient-specific spectral characteristics in local field potential activity.
- Potential for predicting patient-specific, physiology-based stimulation programming.

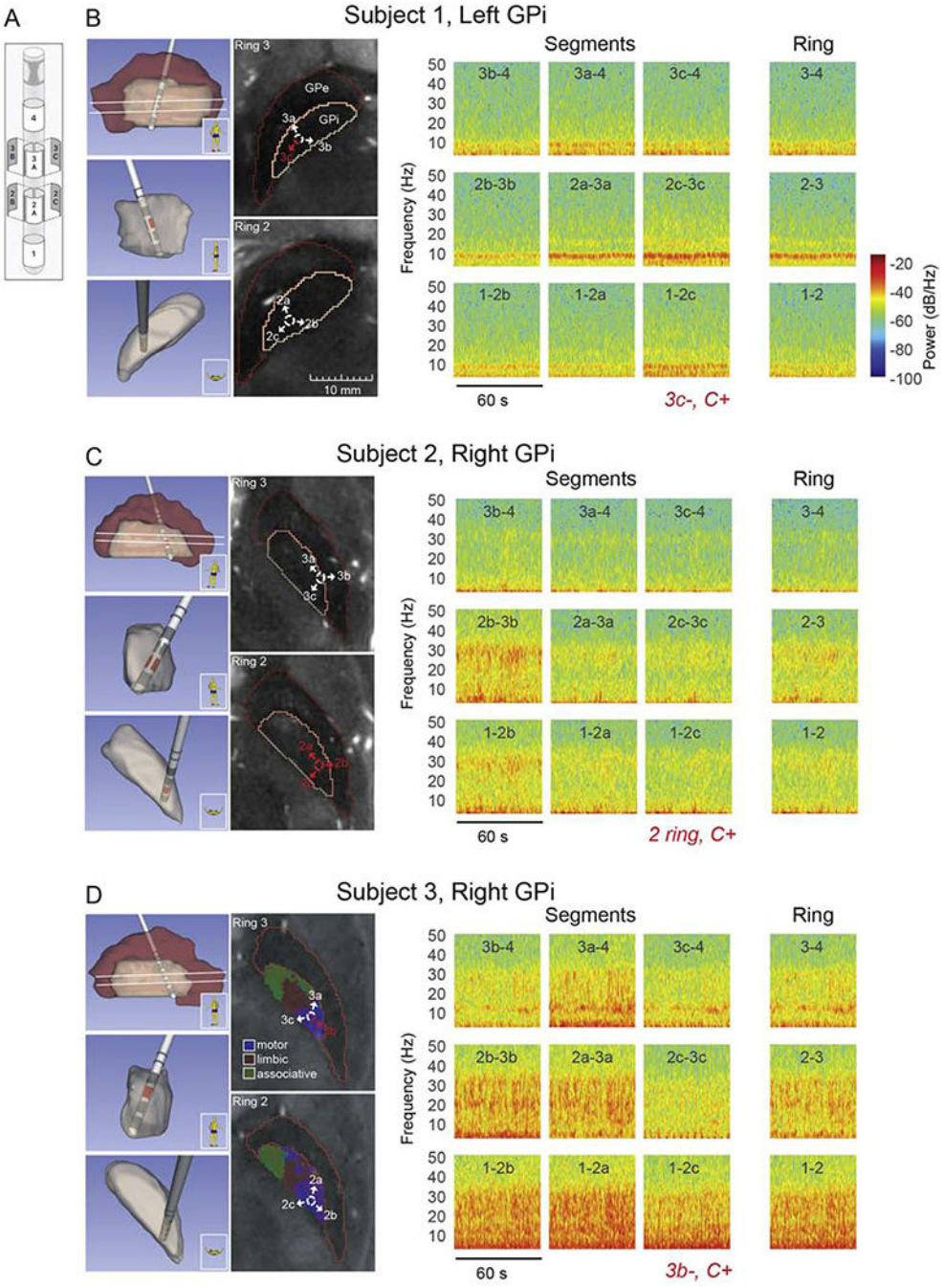

Figure 1. DBS Lead locations and Local Field Potential Topography. [Color; 2-column fitting]

Local field potential recordings in the pallidum of three DBS patients using directional DBS leads. (**A**) Schematic of Abbott Infinity DBS segmented lead (image courtesy Abbott). (**B**) (***left panel)*** Lead and pallidal reconstruction based on pre-operative 7T MRI and post-operative CT scans for subject 1. Sagittal, coronal, and axial views of 3-D reconstructions are shown (top to bottom, respectively). Two axial MRI slices at the levels of segmented contacts (rings 2 and 3, white lines in sagittal 3-D reconstruction) are also shown along with identification of GPi and GPe borders. Labeled arrows corresponding to contact segments

have been added to aid visualization of lead orientation. All axial MRI images in panels (**B-D**) are presented at the same size scale, (***right panel)*** Spectrograms over 60 seconds of spontaneous, resting state LFP activity, comparing directional sensing using segments and ring recordings. The DBS montage selected in clinic during the patient's initial programming visit is shown in red italics. For example '3c−, C+' is monopolar stimulation configuration with segment 3c as the cathode and the battery case as the anode. These settings were chosen by the movement disorder clinician per their standard of care and were blinded to the physiological recordings presented here. Active segments are also indicated in red in lead location reconstructions and axial MR images. (**C,D**) Same as in panel **B**, for subjects 2 and 3, respectively. The axial MRI slices in panel D also include parcellations of motor (blue), associative (green), and limbic (red) territories estimated based on 7T diffusion MRI scans collected in this subject.

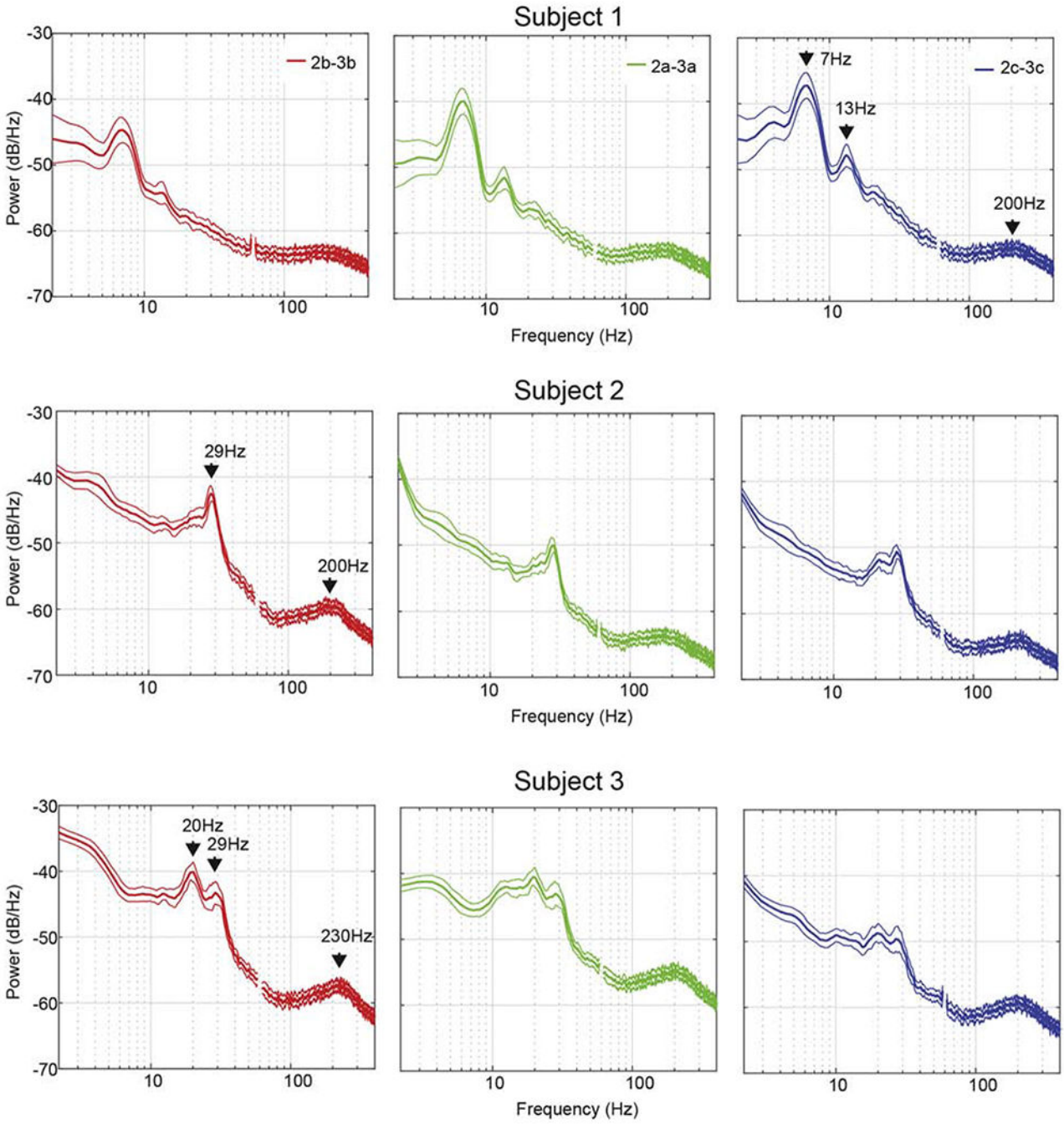

Figure 2. Resting State Power Spectral Density Plots. [1.5 column-fitting]

Power spectral density (PSD) plots of local field potential recorded from the pallidum of three DBS patients. PSD plots were generated from spectrograms calculated over 5 minutes of continuously recorded data collected at rest. Spectrograms were divided into 15-second segments, averaged over time, and the resulting 20 PSD traces were averaged. Mean +/− 2SD are shown. Data presented here are from vertically adjacent segment pairs from rings 2 and 3 (e.g. 2a-3a). For visualization purposes, data points between 58 and 62 Hz (corrupted by line noise) were excluded. For each subject, salient peaks in the PSD were identified and

labeled on the plots identified as having the highest peak in oscillatory power in the 5-35 Hz range.

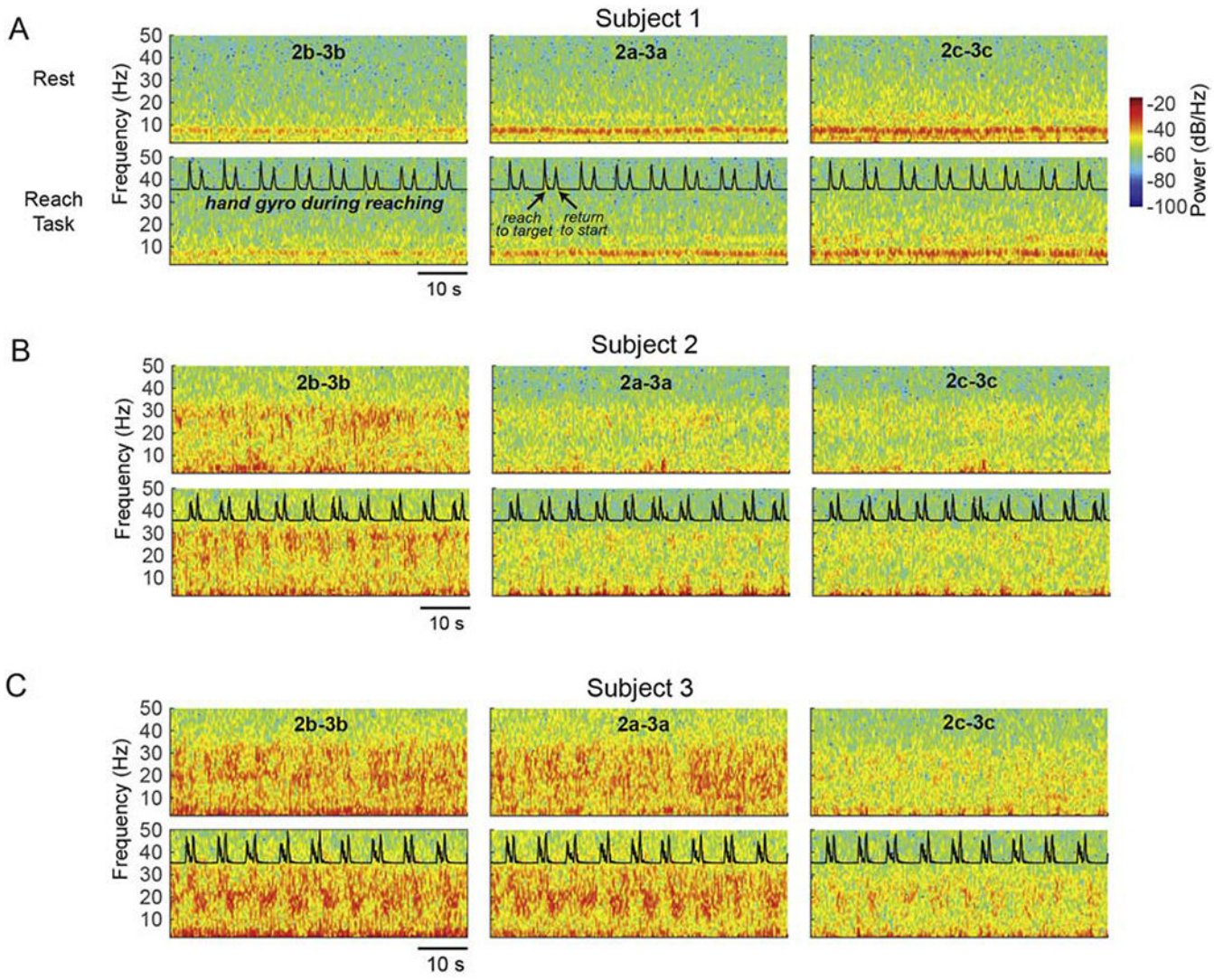

Figure 3. Resting State and Reach Task Spectrogram Plots. [color; 2 column-fitting]

Reach task-related changes in oscillatory activity in the GPi. (**A**) Spectrograms over 60 seconds in two conditions in subject 1: rest (*top row*), touchscreen reaching task (*second row; normalized gyroscope trace collected from a Delsys IMU sensor is overlaid*). Each column represents a bipolar configuration using the vertically adjacent segments of rings 2 and 3 (e.g. 2a-3a), with the same behavioral data overlaid in each column for visualization. (**B,C**) Same as in (**A**) for subjects 2 and 3, respectively. All plots have the same color scale as in panel (**A**).

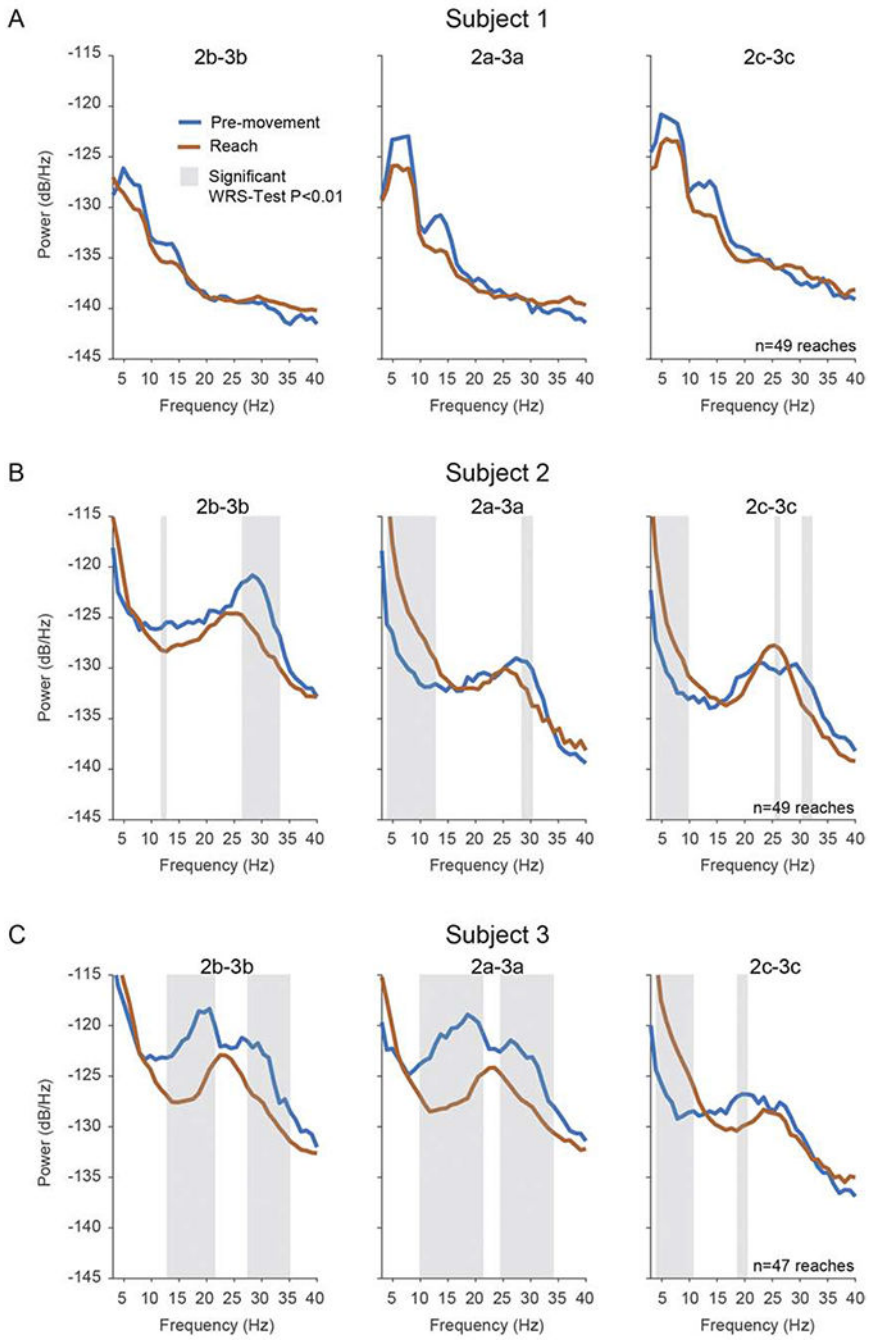

Figure 4. Power Spectral Density Plots of Resting State Compared to Reach Task. [color; 1.5 column-fitting]

The effects of movement on spectral power in the 3-40Hz range in the GPi (**A**) Median PSDs in pre-movement and reach conditions in subject 1. Reach PSDs were calculated during a time period centered at maximal reach velocity (see Methods); pre-movement PSDs were calculated from a time period prior to reaching while the patient maintained a resting position on the startpad. Each column represents a bipolar configuration using the vertically adjacent segments of ring 2 and 3 (e.g. 2a-3a). Shaded regions indicate significant

differences between PSDs based on the Wilcoxon rank-sum (WRS) test (p=0.01) corrected for multiple comparisons. Two consecutive bins had to pass the WRS-test for a difference to be considered significant.

Table 1:

Patient Demographics and Clinical Ratings of Parkinsonian Motor Signs

	Patient ID	UD1015	UD1018	UD1019
	Age/Sex	63 / F	60 / F	52 / M
	Time from diagnosis to recording (yrs)	7	10	6
	Handedness	Right	Right	Right
	DBS side	Left	Right	Right
	Side of disease onset	Right	Left	Left
	Pre-operative prominent features	Dyskinesias, fluctuations, rigidity, tremor, bradykinesia	Rigidity, bradykinesia, gait imbalance	Dyskinesias, fluctuations, freezing, bradykinesia, rigidity, gait disturbance
	Days from surgery to externalized recordings	4	7	5
Total possible	**UPDRS-III**			
12 / 4	**Tremor (UE / LE)**[a]	2 / 3	1 / 0	2 / 0
4 / 4	**Rigidity (UE / LE)**[a]	2 / 2	2 / 3	2 / 2
12 / 8	**Bradykinesia (UE / LE)**[a]	6 / 4	8 / 7	4 / 1
32	**Axial**[c]	9	14	22
44 (132)	**Total Unilateral**[b] **(Total Body**[c]**)**	19 (53)	21 (44)	11 (46)

[a]Tremor, rigidity and bradykinesia sub-scores are reported in accordance with those defined by Goetz et al. (2008) (Goetz *et al.*, 2008) and reported here are unilateral scores (contralateral to the side from which LFPs were recorded) and collected in the off-medication state prior to DBS implantation.

[b]Total Unilateral scores consist of adding Tremor, Rigidity and Bradykinesia (UE & LE) subscores.

[c]Total scores and axial scores reported here include the entire(bilateral) UPDRS-III subscore, in order to give a sense of disease state.